Journal Name

RSCPublishing

ARTICLE

Novel polyoxadiazoles with noncoplanar ortho-linked structures as highly CO_2 permselective membranes

Cite this: DOI: 10.1039/x0xx00000x

E. Abouzari-Lotf,[a,*] A. Shockravi,[b] A. Rafieimanesh,[b] M. Saremi,[b] A. Javadi,[b] M.M. Nasef [a,*]

Received 00th January 2012,
Accepted 00th January 2012

DOI: 10.1039/x0xx00000x

www.rsc.org/

A novel class of polyoxadiazole membranes containing noncoplanar 1,1′-thiobis(2-naphthoxy) (S-BINOL) groups was synthesized using versatile route and tested for CO_2 separation. Dihydrazide monomer was obtained in a two-step high-yielding procedure and used in polycondensation reaction with terephthaloyl chloride to prepare a polyhydrazide, which was converted into amorphous and soluble polyoxadiazoles having an inherent viscosity of around 1 dLg^{-1} by a simple thermal cyclization without using any solvent or in solvent cyclization. The *ortho*-linked sulfide groups of the obtained polymers were subsequently oxydized to yield sulfone-containing polymers. Polyoxadiazole membranes demonstrated comparable CO_2 separation properties to those of the imide based polymers and almost better performance than the commercial and modified polyethersulfones, and the previously reported polyoxadiazoles. The sulfone-containing polyoxadiazole membranes exhibited higher permeability, lower selectivity, and enhanced plasticization pressure than the corresponding sulfide containing ones.

Introduction

Membrane-mediated separations have been emerged as fast-growing separation technologies and became vital component in various energy related applications.[1, 2] Polymeric membranes are the first and most common commercial membranes used for a variety of industrial gas separation processes including O_2/N_2 (e.g., nitrogen generation) and CO_2/CH_4 (e.g., natural gas enrichment). Membrane-based separation processes inherently provides low cost, high energy efficiency, design flexibility, and ease of operation. Among membrane gas separation processes, removal of CO_2 from natural gas is a relatively new technology that is competing with various well-established conventional gas processing technologies such as absorption and adsorption. While there are huge demands and market potentials for membrane based CO_2 separation, the persisting challenge remains in the development of durable membranes with enhanced selectivity and permeability.[3, 4] Therefore, research for advanced polymeric membranes with enhanced permselectivity and sufficient thermal, chemical, and mechanical stability at high temperature and pressure is ever receiving growing attention in the field of membrane science and technology.[5, 6]

As reported by Robeson,[7, 8] there is a general trade-off between the gas permeability and selectivity of polymeric materials. More selective membranes are often less permeable and vice versa. In this regard, several structure-property relationship studies have identified the best combinations of polymer structures resulting in high selectivity and permeability.[7-10] Accordingly, two designing principles have been proposed for improving the selectivity and diffusivity of membranes:[11-14] (i) simultaneous increase in interchain separation (inhibition of intersegmental packing) and decrease in polymer backbone mobility and (ii) weakening interchain interactions to avoid electronic interactions. The introduction of rigid and bulky packing-disrupting units into the backbone has been proposed as the most effective way of enhancing diffusivity and selectivity through hindrance of packing of the relatively rigid backbones and reduction of the rotational mobility around the flexible groups.[15-19]

A large number of polymeric materials including polyimides,[20, 21] poly(amide-imide)s,[22] polybenzimidazoles,[23] polycarbonates,[24] and polysulfones[25] have been investigated and developed as promising membranes for CO_2 separation applications. However, these membranes were found to develop shortcomings including limited thermal and chemical stability together with suffering from the usual trade-off between the desirable properties of selectivity and permeability.

Thermally stable and chemically resistant heteroaromatic polymers such as polyoxadiazoles (**PODs**) and polyhydantoins have been utilized to prepare dense membranes for CO_2 separation since 1994.[26-29] Despite their excellent thermal and chemical stabilities and good mechanical properties complemented by high selectivity and good permeability, application of **POD** membranes in separation technologies were limited by their quite difficult processing and fabrication. Similar to other aromatic rigid polymers, these fully aromatic backbones are not soluble in any organic solvents and exhibit a very high (or no) glass transition temperature. Various attempts have been made to modify the solubility and processability of the rigid chain polymers by introducing either noncoplanar or bulky groups,[30-32] groups with greater rotational freedom such as -O-, $-CH_2-$, $-C(CH_3)_2-$ and $-C(CF_3)_2-$,[33-36] or less symmetric units such as *ortho*- and *meta*-catenated aromatic rings in the main chains.[37-39] Naphthalene is a bulky, rigid and heat resistance moiety.[40-42] As observed in our previous studies, the incorporation of *ortho*-linked

binaphthyl-based systems such as 1,1′-thiobis(2-naphthoxy) (**S-BINOL**) catenate could disrupt the crystal packing, reducing intermolecular interactions and enhancing solubility of the resulting polymers.[43, 44] Considering such observation, it was envisaged that the introduction of the S-**BINOL** catenate to the polyoxadiazole backbone might lead to simultaneous increase in the fractional free volume (FFV) and the rigidity of the polymer. The former leads to higher diffusivity whereas, the latter results in significant selectivity improvement.

In the present study, in order to prepare efficient membranes, relatively rigid polyoxadiazole backbones containing poor chain packing **S-BINOL** and **SO_2-BINOL** catenates were designed and synthesized. The general characteristics of the obtained polymers such as crystallinity, thermal and physical properties were investigated. The performance of the membranes with respect to CO_2 separation under various feed compositions, pressures, and temperatures were also evaluated and presented. A special attention was also given to establish a correlation between the structural variations in the polymer backbone and their impact on the gas transport properties.

Experimental

Materials

1,1' -Thiobis(2-naphthol) (**S-BINOL**) and 1,1' -thiobis(2-naphthoxy acetic ester) (**S-BINOL-DE**) were synthesized according to the procedure reported in a previous communication.[44] Hydrazine monohydrate (Acros), terephthaloyl chloride (Merck) and polyphosphoric acid (PPA, Merck) were used as received. *N*-methyl-2-pyrrolidone (NMP, Merck) and pyridine (Py, Fluka) were purified by distillation under reduced pressure over calcium hydride and stored over 4Å molecular sieves. LiCl (Merck) was dried under vacuum at 180 °C before use.

Synthesis

1,1'-thiobis(2-naphthoxy hydrazide) (S-BINOL-DH)

A mixture of 4.62 g (10 mmol) of **S-BINOL-DE** and 1.4 mL (30 mmol) of hydrazine hydrate was stirred under reflux in methanol for 20 h. After cooling to room temperature, the precipitates were filtered and washed with ethanol repeatedly. White crystalline **S-BINOL-DH** was isolated in 85% of yield after purification by sublimation under vacuum and stored on P_2O_5. mp: 206.4-208.2 °C. ^{1}H NMR (300 MHz, DMSO-d_6, δ): 9.02 (s, 2H, (O=C-N-H), 8.39 (d, 2H, J=8.4 Hz, Ar H), 7.85 (d, 2H, J=9.1 Hz, Ar H), 7.82 (d, 2H, J=8.1 Hz, Ar H), 7.41 (d, 2H, J=8.3 Hz, Ar H), 7.33 (d, 2H, J=9.2 Hz, Ar H), 7.32 (d, 2H, J=8.2 Hz, Ar H), 4.57 (s, 4H, CH_2), 4.33 (s, 4H, NH_2); ^{13}C NMR (75 MHz, DMSO-d_6, δ): 166.34 (C=O), 158.24 (Ar), 135.48 (Ar), 130.32 (Ar), 129.60 (Ar), 128.24 (Ar), 127.34 (Ar), 125.81 (Ar), 123.24 (Ar), 120.02 (Ar), 115.14 (Ar), 65.71 (CH_2); IR (KBr): v = 3306 (s, N-H stretching), 3045 (w, Ar-H stretching), 2925 (w, C-H stretching), 1670 hydrazide I band (s, hydrazide C=O stretching), 1620 hydrazide II band (m, N-H bending), 1530 (w), 1505 (m), 1305 (w), 1265 (s), 1230 (w), 1150 (w), 1075 (w), 1000 (w), 915 (w), 805 (m), 800 (m), 695 (w), 616 (w) cm^{-1}. Anal. Calcd. for $C_{24}H_{22}O_4N_4S$ (%): C 62.32, H 4.79, N 12.11; found, C 62.27, H 4.69, N 11.81.

Polyhydrazide (PH)

A mixture of 4.62 g (10 mmol) of **S-BINOL-DH**, 0.425 g (10 mmol) of LiCl, 1.1 mL of pyridine, and 12 mL of NMP was stirred under nitrogen atmosphere. After the solution became clear, 2.30 g (10 mmol) of terephthaloyl chloride was added. The reaction was carried out for 2 h at 0 °C and 12 h at 80 °C. Subsequently, the obtained highly viscous reaction mixture was poured into 200 ml water. The fiber-like precipitate was collected by filtration and washed several times with water and ethanol and dried in a vacuum oven for 24 h. Yield: 90%; inherent viscosity: 1.17 dLg^{-1}; IR (KBr): v = 3260 (s, N-H stretching), 3055 (w, Ar-H stretching), 2930 (w, C-H stretching), 1660 hydrazide I band (s, hydrazide C=O stretching), 1620 hydrazide II band (m, N-H bending), 1590 (w), 1500 (m), 1460 (w), 1260 (s), 1225 (s), 1150 (w), 1080 (m), 810 (m), 760 (w) cm^{-1}. Anal. Calcd. for $C_{32}H_{24}N_4O_6S$ (%): C 64.85, H 4.08, N 9.45; found, C 64.09, H 4.58, N 9.10.

Cyclodehydration of polyhydrazides

Both thermal and chemical cyclodehydration methods were used to convert polyhydrazides into corresponding polyoxadiazoles of **t-POD** or **t-OPOD** and **s-POD**, respectively. In the first case, the reactions were performed on films under vacuum while in the chemical method, solution of PPA was used for cyclodehydration in an inert atmosphere.

Thermal cyclodehydration. Polyhydrazide films were prepared by dissolving a polymer in DMAc (~6% w/v) and filtering through a 0.45-μm Teflon syringe filter. The filtered solutions were then poured onto a glass plate, followed by drying for 24 h with an infrared lamp and in a vacuum oven at 100 °C for 24 h. The cyclodehydration was performed to yield the corresponding polyoxadiazoles (**t-POD** and **t-OPOD**) by successive heating for 10 h at 200 °C and 2 h at 250 °C under vacuum.

t-POD: inherent viscosity: 1.06 dLg^{-1}; cyclization yield: 95.6% (based on thermal analysis data); IR: v = 3205 (w), 3050 (w, Ar-H stretching), 2940, 1605, 1580 (m, C=N stretching), 1525 (w), 1490 (w), 1230 (m), 1175 (w), 1040 (m), 955 (w), 815 (w), 750 (w) cm^{-1}. Anal. Calcd. for $C_{32}H_{20}N_4O_4S$ (%): C 69.05, H 3.62, N 10.07; found, C 68.31, H 3.81, N 9.70.

t-OPOD: cyclization yield: 95.2% (based on thermal analysis data); IR: v = 3100 (w), 3065 (w, Ar-H stretching), 2930 (w, C-H stretching), 1600 (m), 1580 (m, C=N stretching), 1490 (w), 1315 (w), 1230 (m), 950 (w), 825 (m), 750 (m), 720 (w) cm^{-1}. Anal. Calcd. for $C_{32}H_{20}N_4O_6S$ (%): C 65.30, H 3.45, N 9.50; found, C 64.78, H 3.92, N 9.16.

Chemical cyclodehydration. 2.00 g of **PH** in 35 mL of polyphosphoric acid was heated at 100 °C for 4 h. Then the reaction mixture was slowly poured into the water. The resulting precipitated polymer was collected by filtration, carefully washed with water and ethanol and dried in a vacuum oven for 24 h. The inherent viscosity of **s-POD** was 0.98 dLg^{-1}, measured at a concentration of 0.5 g dL^{-1} in NMP at 30 °C. Cyclization yield: 99.5% (based on thermal analysis data); IR (KBr): v = 3210 (w), 3050 (w, Ar-H stretching), 2935 (w, C-H stretching), 1600 (m), 1580 (m, C=N stretching), 1525 (w), 1495 (w), 1235 (m), 1170 (w), 1040 (w), 1010 (m), 955 (w), 815 (m), 750 (w), 715 (w) cm^{-1}. Anal. Calcd. for $C_{32}H_{20}N_4O_4S$ (%): C 69.05, H 3.62, N 10.07; found, C 68.27, H 3.73, N 9.60.

Oxidation of sulfide to sulfone

General Procedure. A mixture of sulfide containing polymer (2.00 g) in 10 mL glacial acetic acid, and hydrogen peroxide 30% (1.5 mL) was refluxed for 6 hours. Subsequently, water was added and the solid product was filtered, washed with 10% acetic acid/water mixture and hot water then dried in a vacuum oven overnight.

s-OPOD: inherent viscosity: 0.93 dLg^{-1}; IR (KBr): v = 3105 (w), 3060 (w, Ar-H stretching), 2920 (w), 1585 (m, C=N stretching),

1580 (m), 1490 (w), 1315 (m), 1235 (m), 950 (m), 750 (m), 725 (w) cm^{-1}. Anal. Calcd. for $C_{32}H_{20}N_4O_6S$ (%): C 65.30, H 3.45, N 9.50; found, C 64.87, H 3.85, N 9.07%.

OPH: inherent viscosity: 0.98 dLg^{-1}; IR (KBr): ν = 3295 (s, N-H stretching), 3050 (w, Ar-H stretching), 1675 hydrazide I band (s, hydrazide C=O stretching), 1620 hydrazide II band (m, N-H bending), 1595 (w), 1490 (m), 1460 (m), 1317 (w), 1255 (s), 1225 (s), 1080 (m), 810 (m) cm^{-1}. Anal. Calcd. for $C_{32}H_{24}N_4O_8S$ (%): C 61.53, H 3.87, N 8.97; found, C 63.17, H 4.02, N 8.60.

Characterization Techniques

IR spectra were recorded in potassium bromide (KBr) pellets or films on a Perkin Elmer (Perkin Elmer FT spectrum RX1, USA) over the range 400-4000 cm^{-1}. ^1H NMR and ^{13}C NMR spectra were recorded using Bruker DRX AVANCE 300. Elemental analysis performed by a Perkin Elmer 2004 (II) CHN analyzer. Melting points (uncorrected) were measured with an Electrothermal Engineering LTD 9200 apparatus. Inherent viscosities ($\eta_{inh} = \frac{\ln \eta_r}{c}$ at a concentration of 0.5 g dl^{-1}) were measured with an Ubbelohde suspended-level viscometer at 30 °C using NMP as solvent. Thermogravimetric analysis were recorded on a thermal analyzer 931 TA instrument under nitrogen atmosphere at a heating rate of 10 °C min^{-1}. Glass-transition temperatures were measured on a differential scanning calorimetry (DSC) 950 TA analyzer with a heating rate of 10 °C min^{-1}. Tensile strength and elongation at break of thin films were evaluated with a Shimadzu AG-10-TB at room temperature and in 5% strain rate of the sample specimen length. Wide angle X-ray diffraction measurements were recorded at room temperature on a PW 1800 (Philips) over a range of 2θ=4-80°. Based on the Bragg's law, the average *d*-spacing (*d*) was calculated as following

$$d = \frac{n\lambda}{2\sin\theta} \quad (1)$$

where 2θ is the X-ray diffraction angle, λ is wavelength = 1.54 Å, and *n* is an integer number (1, 2, 3…) related to the Bragg order. Generally, the *d* value serve as an indicator of *openness* or free volume available for penetrating gas molecules.

The film density was determined in a $Ca(NO_3)_2$ solution with standard buoyancy method. The following equation was used to calculate the density value.

$$\rho_{film} = \frac{w_{air}}{w_{air} - w_{solvent}} \times \rho_{solvent} \quad (2)$$

where, ρ is density and W is weight which were measured in air and $Ca(NO_3)_2$ solution. The obtained density was used to calculate a dimensionless FFV parameter using equation 3. This equation essentially used to characterize the local available space in a dense polymer chains.

$$FFV = \frac{V_{sp} - V_{oc}}{V_{sp}} \quad (3)$$

where V_{sp} is the specific volume, which is measured experimentally and equals the reciprocal of density, $V = 1/\rho$ (cm^3g^{-1}), and V_{oc} is the occupied volume by polymer chains and can be estimated by Bondi's group contribution method as $V_{oc} = 1.3 \sum V_W$.[45] The V_w is the van der Waals volume of the groups comprising the polymer chain that was calculated based on quantitative structure-activity relationships (QSARs) method using the Hyperchem software, version 7.0.[46] The QSAR functionality uses the atomic radii as supplied by Gavezotti.[47]

Gas separation measurements

The pure and mixed gas permeability coefficients were measured using a constant volume, variable pressure apparatus at different feed pressures and temperatures as described elsewhere.[48] A gas chromatography (8700 Perkin Elmer) equipped with a thermal conductivity detector (GC-TCD) was used to evaluate the concentration of each gas in the permeate side. The permeability of each gas (P_i) was described in Barrer ($cm^3(STP)cm^{-2}.s^{-1}.cmHg^{-1}$) by the following relationship:

$$P_i = \frac{Rl}{A(p_1 - p_2)} \quad (4)$$

where R is the flow rate of gas permeating through the membrane ($cm^3(STP)s^{-1}$), l is the membrane thickness (cm), A is the effective membrane area (cm^2), and p_1 and p_2 are the absolute pressures of the feed and permeate sides (cmHg). The permeability data of two gas species were used to obtain the ideal selectivity of gas i over gas j, $\alpha_{ideal\,(\frac{i}{j})}$, which is defined as the ratio of pure gas permeability of each species.

$$\alpha_{ideal\,(\frac{i}{j})} = \frac{P_i}{P_j} \quad (5)$$

The real selectivity of membranes was calculated with mixed gas as follows:

$$\alpha_{real\,(\frac{i}{j})} = \frac{Y_i/Y_j}{X_i/X_j} \quad (6)$$

where Y and X are the molar fractions of the two gases at the feed and permeate sides, respectively.

Results and discussion

Monomer and polymer synthesis and characterization

The monomer was synthesized in a high purity form **S-BINOL** by a two-step high-yielding procedure as shown in Fig. 1. Firstly, the treatment of **S-BINOL** with methylcholoroacetate gave corresponding diester in 90% yields. Subsequently, the dihydrazide monomer was readily obtained by refluxing of the intermediate diester with the excess of hydrazine hydrate.

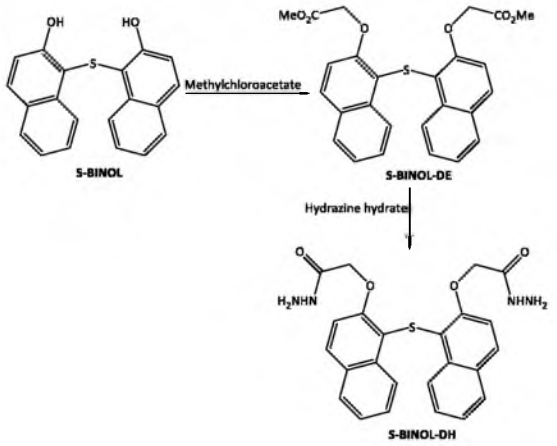

Fig. 1 Monomer synthesis.

The structure of the **S-BINOL-DH** monomer was confirmed by FT-IR, ^1H and ^{13}C NMR, and elemental analysis. Assignments of each proton are assisted in ^1H spectrum and shown in Fig. 2. As could be seen, the data agreed well with the proposed structure of the synthesized monomer. Two resonance signals at most downfield and upfield regions; 9.02 (s, 2H, NH protons) and 4.3 (s, 4H, NH_2 protons) ppm are ascribed to the protons of hydrazide groups (H_i and H_a). Also, the area of integration for protons is in accordance with the assignments.

Polyhydrazides containing **S-BINOL** were synthesized by polycondensation method as described in Fig. 3. In addition to

terephthaloyl chloride monomer, the polymerization of the isophthaloyl chloride with **S-BINOL-DH** was also attempted under various conditions by changing the reaction temperature and time. However, these attempts were not successful and the resulting low molecular weight polymers produced brittle films or films with low mechanical stability. Hence, terephthaloyl chloride based materials were alternatively used for the next experiments.

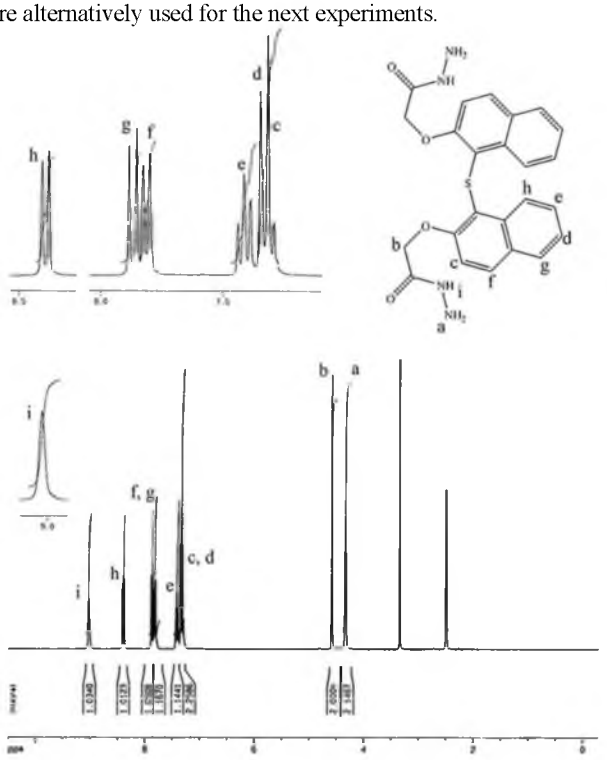

Fig. 2 ^{1}H NMR spectrum of **S-BINOL-DH** in DMSO-d6.

Polyoxadiazoles were prepared by cyclodehydration of polyhydrazide films by thermal treatment or solution method using polyphosphoric acid as a dehydrating agent, according to the route depicted in Fig. 3.

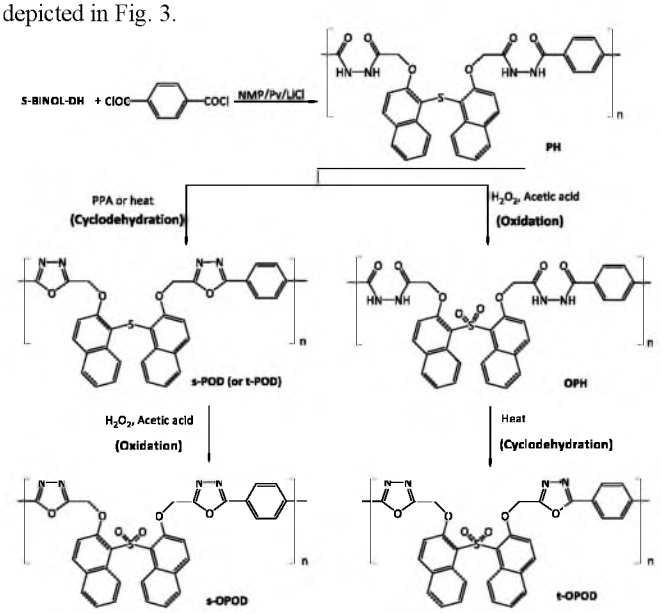

Fig. 3 Synthesis of the polyhydrazides, cyclodehydration, and oxidation to the corresponding sulfone containing polymers.

Upon cyclodehydration, the intensive absorption peaks at around 3200-3300 cm^{-1} due to the N-H stretching and 1670 cm^{-1} arising from carbonyl groups of polyhydrazide were almost disappeared. In addition, the characteristic bands of the oxadiazole ring at 1580, 1010 and 950 cm^{-1} were appeared (Fig. 4). Dehydration to the oxadiazole structure was also confirmed by the CHN elemental analysis. The carbon mass showed more than 4% weight increase due to the dehydration and C 68.27 wt%, H 3.73 wt% and N 9.60 wt% (**s-POD**) is well consistent with the calculated values of C 69.05 wt%, H 3.62 wt% and N 10.07 wt%. The slightly higher contents of hydrogen in CHN data and small peaks above 3200 cm^{-1} in IR can be attributed to the absorbed water or incomplete cyclodehydration.

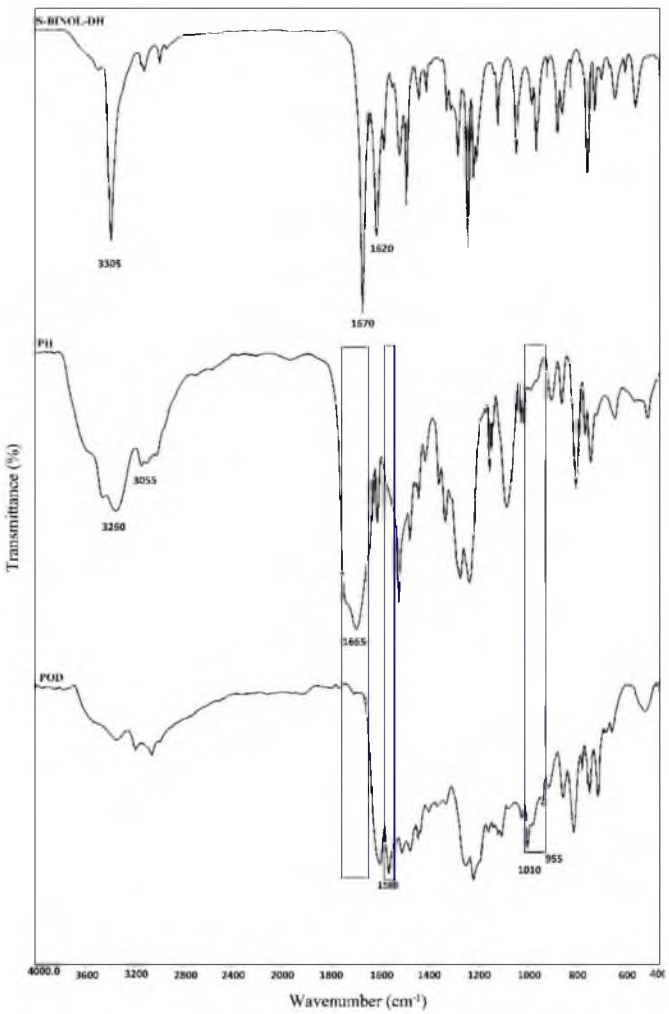

Fig. 4 FT-IR spectrum of **S-BINOL-DH**, corresponding polyhydrazide (**PH**) and chemically cyclodehydrated polyoxadiazole (**POD**).

Since the hydrazide group is considered to be less stable than oxadiazole ring, thermogravimetric data can be used to evaluate the degree of cyclization reaction or the hydrazide content (%HZ).[49] It was determined from the weight loss of residual hydrazide groups of polyoxadiazoles in distinct regions of temperatures between 270 and 325 °C. The following equation was used to calculate the hydrazine content,

$$HZ\ (\%) = \frac{[wl(\%) \times Mw]}{1800 - (18 \times wl(\%))} \qquad (7)$$

where $wl(\%)$ is the related weight loss obtained from the TGA and the Mw is the repeat unit molecular weight of polyoxadiazole (g/mol). With optimization of the cyclization parameters including time and temperature, a hydrazine content of less than 0.5% equal to cyclization yield of more than 99.5% was obtained for the polyoxadiazole cyclized in solution (**s-POD**), as shown in Fig 5. On the other hand, thermally cyclodehydration results in more than 4.1% hydrazide content which is equivalent to cyclization yield of around 95.9%. It is noteworthy mentioning that cyclized films at higher temperatures are brittle and have very low mechanical strength.

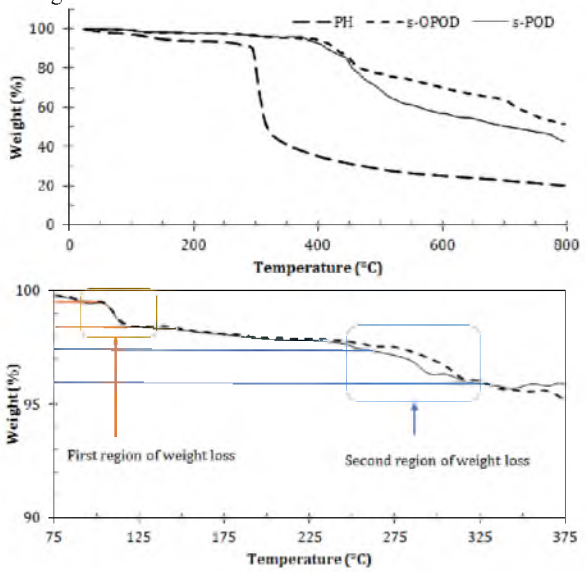

Fig. 5 Thermogravimetric analysis of **PH**, **s-POD** and **s-OPOD** (top) and expanded regions of distinct weight losses in **PODs** (down) under N_2 atmosphere at a heating rate of 10 °C min^{-1}.

Finally, the sulfide group of polyoxadiazole and polyhydrazide readily oxidized into sulfone by means of hydrogen peroxide. Although the symmetric stretching band of sulfone group is not a good indicator for this oxidation due to its overlap with other absorption bands, the asymmetric band at around 1315 cm^{-1} clearly confirms the oxidation. In addition, elemental analysis shows good agreement with the expected values for oxidation. Based on the agreement between calculated and found data, introducing of sulfone group through oxidation of polyoxadiazole is preferred to oxidation of polyhydrazide.

X-ray diffraction and solubility of the polymers

Wide-angle X-ray diffraction patterns were used to investigate the morphology of the polyoxadiazoles and morphological differences between the sulfide and sulfone bridged arrangements. As shown in Fig. 6, the curves of both polyoxadiazoles were broad and without obvious peak features, indicating their amorphous structure. This amorphous nature can be mainly attributed to the presence of the noncoplanar *ortho*-linked structure in the polymer backbone which hinder efficient chain packing and decrease the regularity through weakening intermolecular forces between the polymer chains; subsequently causing a decrease in crystallinity.
The structural noncoplanarity and cisoid conformation of the two naphtyl rings is also evident from the geometry of the **S-BINOL** monomer; optimized with MM2 method using the ChemBio3D Ultra 11.0, shown in Fig. 7 and X-ray structure.[42, 50]

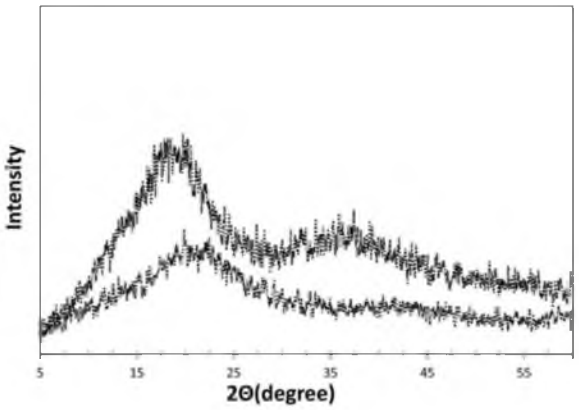

Fig. 6 WAXD patterns of **s-OPOD** (top) and **s-POD** membranes.

The WAXD data could also be used to calculate the average *d*-spacing of a polymer matrix according to the equation 4 (Table 1). The higher *d*-spacing value means more intermolecular distances and therefore more easily passing of penetrant molecules. Since the bridged sulfone group in the *ortho*-position causes more steric repulsion between two naphtyl groups on **BINOL** catenate, the rotational energy barrier around this bond will further increase (shows higher FFV). The XRD patterns in Fig. 6 and *d*-spacing values in Table 1 support the idea of decreased chain stacking resulting from oxidation of sulfide atom in the polymer backbone. This decreased planarity along with the polymer backbone would increase FFV and facilitate the gas permeation through the membrane.

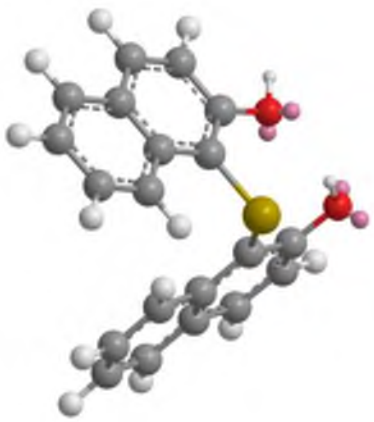

Fig. 7 Geometry optimized structure of the **S-BINOL** monomer.

As shown in Fig. 6, the **POD** shows a maximum peak at about 2Θ = 20.7°, corresponding to an average inter-segmental distance of 4.28 Å; after oxidation, this peak shifts to the left to 2Θ = 17.6°, suggesting the presence of a higher average distance around 0.85 Å in **OPOD**. Meanwhile, the **OPOD** shows a small broad shoulder on the high-angel side at 37° corresponding to a *d*-spacing of 2.42 Å. Based on the similar observations for polyimides [51-53], this halo could be assigned to π-π stacking of oxadiazole and naphthyl rings in ordered domains. Existing of such stacking in sulfone containing polymers confirm the more rigidity of their backbones than corresponding sulfide bridged analogues.

TABLE 1 Physical properties, permeability coefficients, and ideal selectivity of membranes at 30 °C and 9 bar feed pressure

Polymer	Mechanical properties		*d*-spacing (Å)	V_w cm^3g^{-1}	ρ g cm^{-3}	*FFV*	P (barrers)		α_{ideal} $\left(\frac{P_{CO_2}}{P_{CH_4}}\right)$
	Tensile strength (MPa)	Elongation at break (%)					CO_2	CH_4	
PH	32.77	8.15	NA	NA	NA	NA	NA	NA	NA
OPH	30.46	7.94	NA	NA	NA	NA	NA	NA	NA
s-POD	21.16	5.46	4.28	0.538	1.216	0.150	8.04	0.09	89.33
t-POD	8.42	2.60	4.25	0.538	1.215	0.151	9.63	0.18	53.50
s-OPOD	20.68	4.21	5.13	0.547	1.137	0.192	18.75	0.26	72.11
t-OPOD	8.01	2.67	5.06	0.547	1.137	0.192	15.52	0.31	50.06

TABLE 2 Viscosity, solubility,[a] and thermal properties of polymers

Polymer	Viscosity[b]	Solvent[c]						Thermal stability (°C)	
	η_{inh} (dl g^{-1})	NMP	DMAc	DMSO	DMF	THF	$CHCl_3$	T_g[d]	T_{10}[e]
PH	1.17	++	++	++	++	±	-	155	295
OPH	0.98	++	++	++	++	±	-	162	295
s-POD	0.98	++	++	+	±	-	-	245	410
t-POD	1.06	+	±	±	-	-	-	273	400
s-OPOD	0.93	++	++	±	-	-	-	274	425
t-OPOD	-[f]	±	±	-	-	-	-	275	405

(++) Soluble at room temperature, (+) Soluble after heating, (±) partially soluble, (-) insoluble

[a]Measured at a polymer concentration of 0.05 g mL^{-1}.

[b]Measured at a polymer concentration of 0.5 g dL^{-1} in NMP solvent at 30 °C.

[c]NMP: N-methyl-2-pyrrolidone; DMAc: N,N-dimethyl acetamide; DMF: N,N-dimethylformamide; DMSO: dimethyl sulfoxide; THF: tetrahydrofuran.

[d]Midpoint temperature of baseline shift on the DSC heating trace.

[e]Temperature at which 10% weight loss occurred under nitrogen atmosphere.

[f]Could not be measured due to the insolubility in the tested solvents.

Solubility of the high performance polymers is a critical factor that exhibits its processability for diverse applications. The solubility behavior of these amorphous polyhydrazides and polyoxadiazoles was tested and the obtained data was reported in Table 2. The polymers were found to be soluble in highly polar solvents such as NMP, DMAc, and DMSO, at room temperature or upon heating. Such good solubility behavior was probably attributed to the disturbed dense chain packing of the polymer chain by the bulky **S-BINOL**; consequently, the solvent molecules were able to solubilize the polymer chains. As can be seen, the solubility varied depending on the bridged atoms between aromatic rings. Polyoxadiazoles derived from sulfide bridged monomer showed improved solubility. In fact, the presence of sulfur linkages in the backbone further increased the overall flexibility and this polymer was found to be even partially soluble in DMF.

Thermal and mechanical properties

The thermal properties of the polymers, which were evaluated by TGA and DSC techniques, are summarized in Table 2. The DSC analysis shows that there is no evidence of crystallization and melting processes. Therefore, the polymers are in an amorphous state and do not reveal any tendency to crystallize, even in the cooling step. The glass transition temperature of polymers was slightly increased after oxidation, which might be caused by the less flexibility of the sulfone linkages.

As shown in Fig. 5, the polyoxadiazole membrane exhibited good thermal stability and the temperature for 10% weight loss (T_{10}) was above 400 °C. Therefore, it can be concluded that the introduction of flexible ether and methylene linkages and **S-BINOL** catenate did not deteriorate significantly the thermal stability of polyoxadiazoles. They exhibited two distinct transition regions of minor weight loss below 400 °C in nitrogen atmosphere. The first transition occurring between 100-130 °C is associated with the loss of adsorbed water in the polymer. The second transition with an approximate weight loss of less than 2% was positioned in the temperature range of 270 and 325 °C and was due to the loss of water produced during the formation of oxadiazole rings of residual hydrazide groups. This was confirmed by detecting major weight loss for polyhydrazide in the same range of temperature (around 300 °C, Fig. 5). The main region of weight loss associated with the degradation of the main chain was above 410 °C for **POD**. This weight loss temperature was slightly shifted toward higher temperature (above 425 °C) after oxidation.

Table 1 shows the mechanical properties of the membranes; as can be seen, the tensile strength of polyoxadiazoles is above 20 MPa and elongation at break is in the range of 4-6 (%). After converting sulfide to sulfone group, less force per unit area (tensile strength) is required to break the chains apart; it seems that the intermolecular forces between polymer chains decreased in **OPOD**.

Gas Transport Properties

Pure gas

The pure gas permeability and selectivity of the prepared membranes at 30 °C and 9 bar feed pressure are summarized in Table 1. It is well known that gas permeability strongly depends on the fractional free volume of the polymers. Based on the listed FFV in Table 1, the **OPOD** membrane has higher FFV than corresponding sulfide-containing membrane. It could be concluded that the presence of flexible sulfide linkage within a polymer backbone results in an increase in the overall chain flexibility and denser packing compared

to bulky sulfone linkage. However, oxidation led to a sharp increase in the permeability of the membrane due to a decrease in the chain flexibility, loser packing and resulting higher FFV. On the other hand, the higher FFV values obtained upon sulfur oxidation considerably lowered the selectivity values. The data also indicated that the cyclodehydrated membranes in the solution (**s-POD** and **s-OPOD**) show higher selectivity than that of thermally cyclized one.

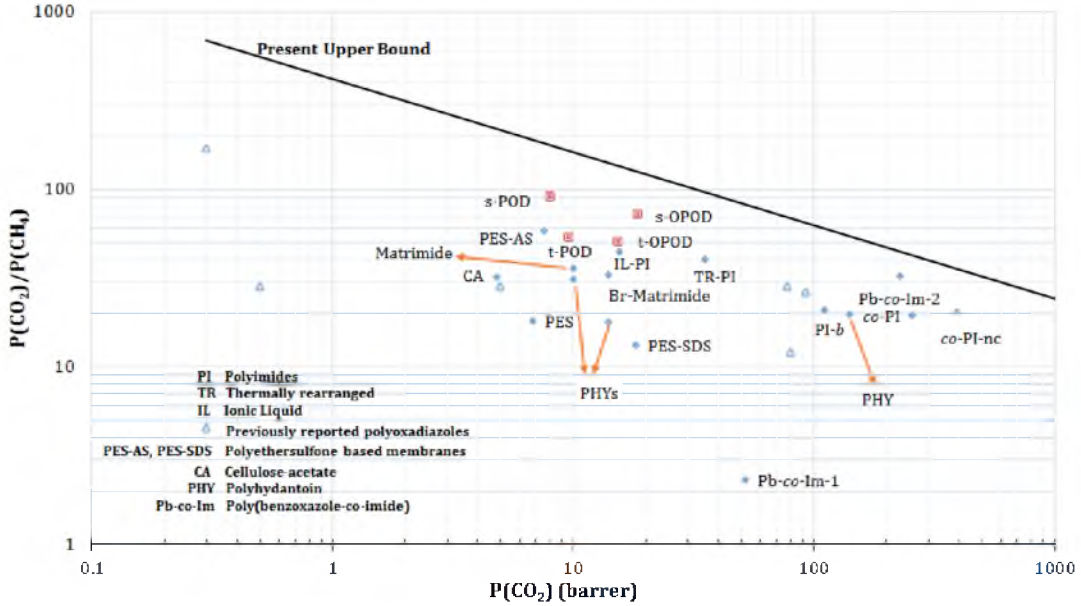

Fig. 8 Comparison of CO_2/CH_4 selectivity *vs* CO_2 permeability of synthesized membranes with some recently important published data including PES and PES-SDS,[48] PES-AS,[54] cellulose-acetate,[55] polyimides and related composite,[56] Matrimide,[57] brominated Matrimid,[58] poly(benzoxazole-co-imide)s,[59] ionic liquid based copolyimide,[60] thermally rearranged PI,[61] PI with bulky group,[18] polyhydantoins (PHYs),[29] and some previously reported polyoxadiazoles shown by triangle.[26, 27]

The comparison of these data with some recently reported polymeric membranes for gas separation is represented in Robeson plot as depicted in Fig. 8. As shown, the gas separation performances of all membranes are below the current Robeson's upper bound. The polyoxadiazole membranes demonstrated almost higher selectivity and in some cases even better CO_2 permeability in comparison to the previously reported polyoxadiazoles[26, 27] and polyhydantoins[29] containing materials. This is coupled with their much higher solubility (as they are soluble in polar aprotic solvents) and therefore better processability than that of previously reported polyoxadiazoles. Upon comparision with pristine and modified polyethersulfones (PESs),[48, 54] current membranes exhibited higher permeability and higher selectivity. Comparison with some recently reported modified polyimides (PI),[56] matrimides,[57, 58] poly(benzoxazole-co-imide)s,[59] ionic liquids based copolyimides,[60] thermally rearranged PI (TR-PI),[61] and PI with bulky group[18] indicated that the present membranes exhibited good performances in CO_2 separations. Particularly, **POD** membranes showed lower CO_2 permeability and higher selectivity than those of previously mentioned imide based polymers.

Mixed CO_2/CH_4 gas

The membrane permeability and selectivity were further tested with mixed binary gas mixtures under various operational temperatures (ranging from 25 to 45 °C), feed compositions (10-75% CO_2), and pressures (5-19 bar). Membranes obtained by cyclization in solution (**s-POD** and **s-OPOD**) were selected for these future evaluations due to their better gas separation properties along with the balance in their mechanical and film-forming properties as described in Table 1. The results are summarized in Figs. 9-11.

As seen in Fig. 9, the increase in CO_2 volume percent in the feed led to a linear increase in the permeability of CO_2. An opposite behavior was observed in selectivity as higher CO_2 concentrations in the feed caused appreciably lower selectivity values. Such observed selectivity is due to the increase in the plasticization effect of CO_2 with increasing its concentration in the feed and consequent larger free volume of membranes.

As could be seen, the slope of this change is different in both membranes. While the sulfide-containing membrane shows negligible increase in the permeability and decrease in the selectivity with the increase in CO_2 concentration in the feed, the sulfone-containing membranes revealed sharper changes with the variation in the feed composition. For instance, when the CO_2 concentration in the feed increased from 25 to 50 %, the CO_2 and CH_4 permeabilities increased by 22 and 43% in **OPOD** and 8.25 and 10% in **POD**, respectively. This was accompanied by a decrease in the selectivity by 15% in the sulfone-containing membranes (**OPOD**) compared to 1.6 % in **POD** membranes.

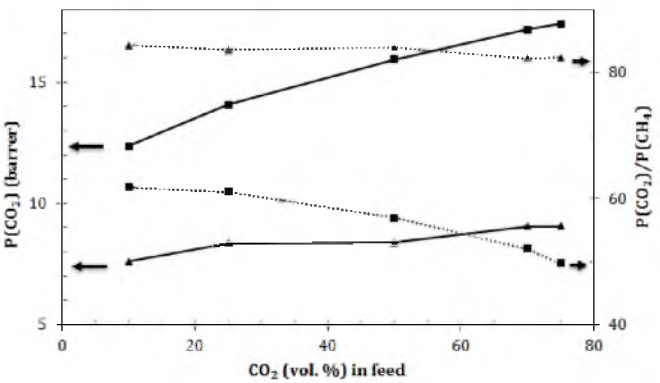

Fig. 9 Feed dependence of CO_2 permeance and CO_2/CH_4 selectivity of **POD** (▲) and **OPOD** (■). Test conditions: 9 bar feed pressure and 30 °C.

To investigate the temperature dependency of permselectivity, the effect of feed temperature on selectivity and permeability of membranes were investigated. The effect of temperature on the gas permselectivity can be generally understood by considering the temperature dependency of gas diffusivity and solubility. The diffusion of gas molecules can be described by the Arrhenius equation.[62] Since the activation energy of the diffusion is mostly positive in glassy polymers, the increase of the feed temperature always increases the gas diffusivity.[54] This activation energy (which is an amount of required energy to sufficiently separate polymer chains to allow penetration) is directly related to penetrant size. For example, in gases with higher diffusion diameters such as CH_4 (3.817 Å), higher activation energy is needed compared with the gases with lower diffusion diameters such as CO_2 (3.325 Å).[62] On the other hand, gas solubility in glassy polymers is directly proportional to the Lennard–Jones temperature of the gas and is fairly insensitive to the chemical structure of the polymer, as suggested by Van Krevelen.[63] Taking the Lennard–Jones temperature into consideration, CO_2 has higher selectivity than CH_4.
As shown in Fig. 10, the increase in the temperature in the range of 25-45 °C caused an increase in the gas permeance in both membranes which is in accordance with the above theoretical discussion. Since CH_4 has higher activation energy than CO_2 and the polymer chains exhibit more mobility in the higher temperatures, the increase in the feed temperature increases permeability of CH_4 more than that of CO_2, resulting in lower selectivity upon increase in the temperature.
An increase in feed pressure can entail two competing effects in glassy polymers: a decrease in the gas permeability due to the saturation of Langmuir sites and an increase in the gas permeability at plasticization pressure.[56] Membrane plasticization is an undesired process usually observed at high feed partial pressure, which increases the permeance and significantly reduces the selectivity. Fig. 11 shows the permeability and selectivity of mixed CO_2/CH_4 gases (50/50) as a function of feed pressure. As can be seen, the increase in the feed pressure up to 15 bar led to a decrease in the permeability coupled with an increase in the selectivity. Both membranes show some degrees of plasticization phenomenon at a CO_2 feed pressure of above 15 bar. It can be concluded that the oxidated (sulfone-containing) membrane displays enhanced plasticization resistance against CO_2, possibly due to the lower degree of chain mobility.

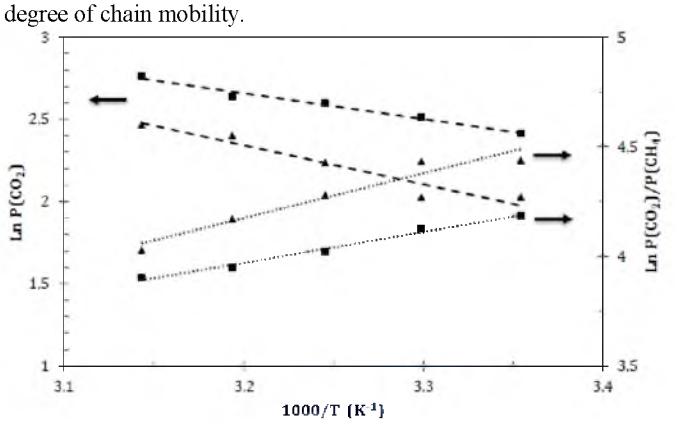

Fig. 10 Temperature dependence of CO_2 permeance and CO_2/CH_4 selectivity of **POD** (▲) and **OPOD** (■). Test conditions: 9 bar feed pressure, 10/90 CO_2/CH_4.

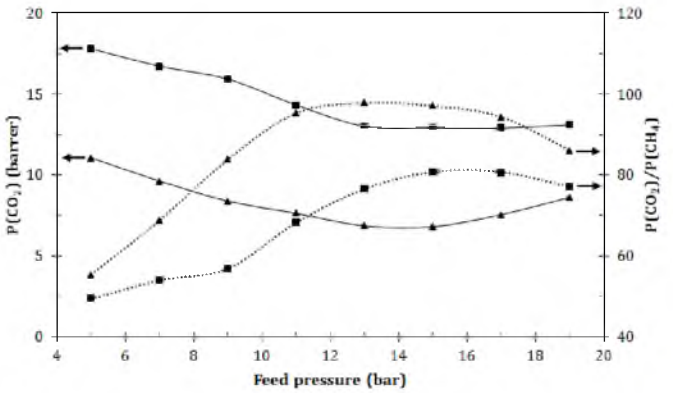

Fig. 11 Effect of feed pressure on CO_2 permeance and CO_2/CH_4 selectivity of **POD** (▲) and **OPOD** (■) membranes. Test conditions: 50/50 CO_2/CH_4, 30 °C.

Conclusions

Novel dihydrazide monomer containing an *ortho*-catenated non-coplanar **S-BINOL** was designed, synthesized, and used as a new building block of polyoxadiazole membranes with high FFV. The incorporation of less symmetric *ortho*-linked and bulky nature of **S-BINOL** reduced the polymer backbone symmetry, regularity, and chain packing efficiency which resulted in substantially improved solubility in polar aprotic solvents, decreased crystallinity and high FFV. The thermal stability showed T_{10} at above 400 °C and membrane recorded a respective ideal selectivity of more than 82% and permeances of 8.04 and 0.09 (barrer) for CO_2 and CH_4, respectively. Oxidation of the sulfide linkage caused a remarkably improved CO_2 permeability (around 18.75 barrer) and lower CO_2/CH_4 selectivity (around 72%). These changes are in accordance with the calculated data for free volume available for penetrating gas molecules (*d*-spacing) and local available space in a dense polymer chains (FFV); oxidation caused a significant increase in the FFV and *d*-spacing of the polymer. In performance evaluation with binary mixed gases, the oxidated membrane displayed an enhanced plasticization resistance against CO_2 and its performance was more sensitive to the change in the feed pressure and composition. Even though these new polyoxadiazole membranes demonstrate better performance than the commercial and modified polyethersulfones and previously reported polyoxadiazoles, the permeability of these membranes still remains lower than that of thermally rearranged (TR) polymers. By the way, their remarkably higher selectivity and inherent stability opens important approach for further improvement in gas separation properties of the polymeric membranes.

Notes and references

[a] Institute of Hydrogen Economy, Energy Research Alliance, International Campus, Universiti Teknologi Malaysia, 54100 Kuala Lumpur, Malaysia.
[b] Faculty of Chemistry, Kharazmi University, Mofatteh Ave. No.49, Postal Code 15614, Tehran, Iran.
* Corresponding authors: Ebrahim Abouzari-Lotf (E-mail: ebrahim@ic.utm.my); Mohamed Mahmoud Nasef (E-mail: mahmoudeithar@cheme.utm.my)

1. A. Koltuniewicz, in *Comprehensive Membrane Science and Engineering*, eds. D. Editor-in-Chief: Enrico and G. Lidietta, Elsevier, Oxford, 2010, pp. 109-164.
2. M. G. Buonomenna, *RSC Advances*, 2013, **3**, 5694-5740.

3. D. D. Iarikov and S. Ted Oyama, in *Membrane Science and Technology*, eds. S. T. Oyama and M. S.-W. Susan, Elsevier, 2011, vol. Volume 14, pp. 91-115.
4. S. D. Kenarsari, D. Yang, G. Jiang, S. Zhang, J. Wang, A. G. Russell, Q. Wei and M. Fan, *RSC Advances*, 2013, **3**, 22739-22773.
5. D. Freeman Benny and I. Pinnau, in *Advanced Materials for Membrane Separations*, American Chemical Society, 2004, vol. 876, ch. 1, pp. 1-23.
6. P. Bernardo, E. Drioli and G. Golemme, *Industrial & Engineering Chemistry Research*, 2009, **48**, 4638-4663.
7. L. M. Robeson, *Journal of Membrane Science*, 1991, **62**, 165-185.
8. L. M. Robeson, *Journal of Membrane Science*, 2008, **320**, 390-400.
9. D. F. Sanders, Z. P. Smith, R. Guo, L. M. Robeson, J. E. McGrath, D. R. Paul and B. D. Freeman, *Polymer*.
10. B. D. Freeman, *Macromolecules*, 1999, **32**, 375-380.
11. M. Langsam and W. F. Burgoyne, *Journal of Polymer Science Part A: Polymer Chemistry*, 1993, **31**, 909-921.
12. W. J. Koros and D. R. B. Walker, *Polym J*, 1991, **23**, 481-490.
13. D. F. Sanders, Z. P. Smith, R. Guo, L. M. Robeson, J. E. McGrath, D. R. Paul and B. D. Freeman, *Polymer*, 2013, **54**, 4729-4761.
14. J. K. Adewole, A. L. Ahmad, S. Ismail and C. P. Leo, *International Journal of Greenhouse Gas Control*, 2013, **17**, 46-65.
15. S. K. Sen and S. Banerjee, *Journal of Membrane Science*, 2010, **365**, 329-340.
16. C. Y. Soo, H. J. Jo, Y. M. Lee, J. R. Quay and M. K. Murphy, *Journal of Membrane Science*, 2013, **444**, 365-377.
17. Z. Liu, B. Liu, L. Li, Y. Zhang and Z. Jiang, *Macromol. Res.*, 2013, **21**, 608-613.
18. M. Calle, C. García, A. E. Lozano, J. G. de la Campa, J. de Abajo and C. Álvarez, *Journal of Membrane Science*, 2013, **434**, 121-129.
19. P. Bandyopadhyay, D. Bera and S. Banerjee, *Separation and Purification Technology*, 2013, **104**, 138-149.
20. S. Sridhar, R. S. Veerapur, M. B. Patil, K. B. Gudasi and T. M. Aminabhavi, *Journal of Applied Polymer Science*, 2007, **106**, 1585-1594.
21. S. Kumar Sen and S. Banerjee, *RSC Advances*, 2012, **2**, 6274-6289.
22. P. Bandyopadhyay, D. Bera, S. Ghosh and S. Banerjee, *Journal of Membrane Science*, 2013, **447**, 413-423.
23. S. C. Kumbharkar, P. B. Karadkar and U. K. Kharul, *Journal of Membrane Science*, 2006, **286**, 161-169.
24. M. Aguilar-Vega and D. R. Paul, *Journal of Polymer Science Part B: Polymer Physics*, 1993, **31**, 1599-1610.
25. K. J. Lee, J. Y. Jho, Y. S. Kang, J. Won, Y. Dai, G. P. Robertson and M. D. Guiver, *Journal of Membrane Science*, 2003, **223**, 1-10.
26. E. R. Hensema, M. E. R. Borges-Sena, M. H. V. Mulder and C. A. Smolders, *Gas Separation & Purification*, 1994, **8**, 149-160.
27. M. E. Sena and C. T. Andrade, *Polymer Bulletin*, 1995, **34**, 643-648.
28. C. H. Jung, J. E. Lee, S. H. Han, H. B. Park and Y. M. Lee, *Journal of Membrane Science*, 2010, **350**, 301-309.
29. R. Tejero, Á. E. Lozano, C. Álvarez and J. de Abajo, *Journal of Polymer Science Part A: Polymer Chemistry*, 2013, **51**, 4052-4060.
30. E. Abouzari-Lotf, A. Shockravi and A. Javadi, *Polymer Degradation and Stability*, 2011, **96**, 1022-1028.
31. A. Shockravi, E. Abouzari-Lotf and A. Javadi, *Designed Monomers and Polymers*, 2009, **12**, 119-128.
32. Y. Liu, Y. Zhang, Q. Lan, Z. Qin, S. Liu, C. Zhao, Z. Chi and J. Xu, *Journal of Polymer Science Part A: Polymer Chemistry*, 2013, **51**, 1302-1314.
33. A. Shockravi, E. Abouzari-lotf, A. Javadi and S. Taheri, *Polym. J*, 2009, **41**, 174-180.
34. Y. Zhang, P. Luo, H. Yao and S. Guan, *Reactive and Functional Polymers*, 2012, **72**, 621-626.
35. J. Abajo and J. G. Campa, in *Progress in Polyimide Chemistry I*, ed. H. R. Kricheldorf, Springer Berlin Heidelberg, 1999, vol. 140, ch. 2, pp. 23-59.
36. A. Ghosh, S. K. Sen, S. Banerjee and B. Voit, *RSC Advances*, 2012, **2**, 5900-5926.
37. A. Shockravi, S. Mehdipour-Ataei, E. Abouzari-Lotf and A. Yousefi, *European Polymer Journal*, 2006, **42**, 133-139.
38. J. M. García, F. C. García, F. Serna and J. L. de la Peña, *Progress in Polymer Science*, 2010, **35**, 623-686.
39. H. Kiani, M. Nasef, A. Javadi, E. Abouzari-Lotf and F. Nemati, *J Polym Res*, 2013, **20**, 1-12.
40. J. Ghim, H.-S. Shim, B. G. Shin, J.-H. Park, J.-T. Hwang, C. Chun, S.-H. Oh, J.-J. Kim and D.-Y. Kim, *Macromolecules*, 2005, **38**, 8278-8284.
41. D.-J. Liaw, F.-C. Chang, M.-k. Leung, M.-Y. Chou and K. Muellen, *Macromolecules*, 2005, **38**, 4024-4029.
42. A. Shockravi, A. Javadi and E. Abouzari-Lotf, *RSC Advances*, 2013, **3**, 6717-6746.
43. A. Shockravi, A. Javadi and E. Abouzari-Lotf, *Polym J*, 2011, **43**, 816-825.
44. A. Shockravi, S. Mehdipour-Ataei, E. Abouzari-Lotf and M. Zakeri, *European Polymer Journal*, 2007, **43**, 620-627.
45. A. Bondi, *The Journal of Physical Chemistry*, 1964, **68**, 441-451.
46. , Hypercube Inc., Gainesville, Florida, version 7.0 edn., 2002, vol. version 7.0.
47. A. Gavezzotti, *Journal of the American Chemical Society*, 1983, **105**, 5220-5225.
48. S. Saedi, S. S. Madaeni, A. Arabi Shamsabadi and F. Mottaghi, *Separation and Purification Technology*, 2012, **99**, 104-119.
49. D. Gomes, J. C. Pinto and C. Borges, *Polymer*, 2003, **44**, 6223-6233.
50. J. T. Mague, M. S. Balakrishna, B. Punji and D. Suresh, *Acta Crystallographica Section C*, 2007, **63**, o487-o488.
51. R. Pan, T. Zhou, A. Zhang, W. Zhao and Y. Gu, *Journal of Polymer Science Part B: Polymer Physics*, 2010, **48**, 2257-2261.
52. M. Calle, A. E. Lozano, J. de Abajo, J. G. de la Campa and C. Álvarez, *Journal of Membrane Science*, 2010, **365**, 145-153.
53. J. Wakita, S. Jin, T. J. Shin, M. Ree and S. Ando, *Macromolecules*, 2010, **43**, 1930-1941.
54. S. Saedi, S. S. Madaeni, F. Seidi, A. A. Shamsabadi and S. Laki, *International Journal of Greenhouse Gas Control*, 2013, **19**, 126-137.
55. A. C. Puleo, D. R. Paul and S. S. Kelley, *Journal of Membrane Science*, 1989, **47**, 301-332.
56. M. Askari and T.-S. Chung, *Journal of Membrane Science*, 2013, **444**, 173-183.
57. T. T. Moore and W. J. Koros, *Journal of Applied Polymer Science*, 2007, **104**, 4053-4059.

58. M. D. Guiver, G. P. Robertson, Y. Dai, F. Bilodeau, Y. S. Kang, K. J. Lee, J. Y. Jho and J. Won, *Journal of Polymer Science Part A: Polymer Chemistry*, 2002, **40**, 4193-4204.
59. C. A. Scholes, C. P. Ribeiro, S. E. Kentish and B. D. Freeman, *Journal of Membrane Science*, 2014, **450**, 72-80.
60. P. Li and M. R. Coleman, *European Polymer Journal*, 2013, **49**, 482-491.
61. D. F. Sanders, Z. P. Smith, C. P. Ribeiro Jr, R. Guo, J. E. McGrath, D. R. Paul and B. D. Freeman, *Journal of Membrane Science*, 2012, **409–410**, 232-241.
62. B. W. Rowe, L. M. Robeson, B. D. Freeman and D. R. Paul, *Journal of Membrane Science*, 2010, **360**, 58-69.
63. D. W. Van Krevelen and K. Te Nijenhuis, in *Properties of Polymers (Fourth Edition)*, Elsevier, Amsterdam, 2009, pp. 655-702.

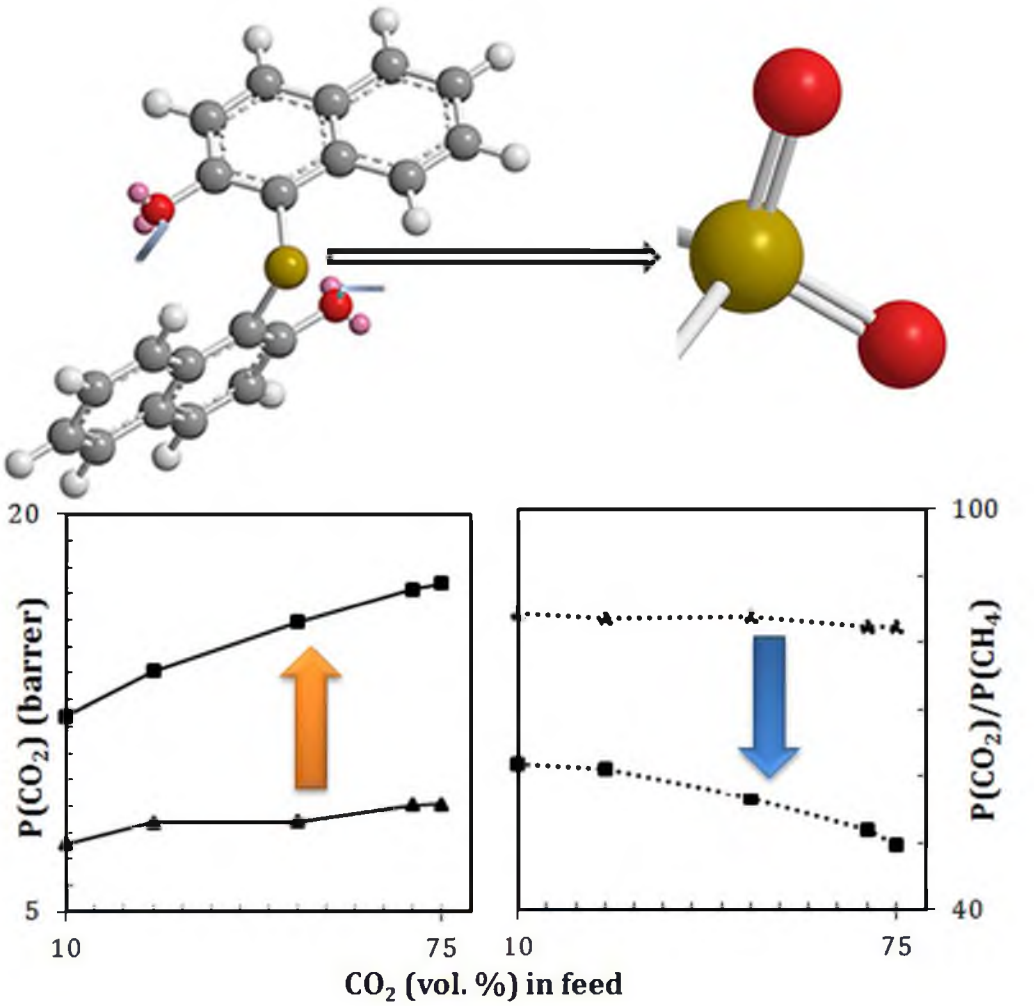

50x50mm (300 x 300 DPI)